Progress In Electromagnetics Research C, Vol. 14, 89–101, 2010

A MICROSTRIP SMALL-SIZED ARRAY ANTENNA BASED ON THE META-MATERIAL ZEROTH-ORDER RESONATOR

A. A. Fashi, M. Kamyab, and M. Barati

Electrical Engineering Department
K. N. Toosi University of Technology (KNTU)
Seyedkhandan, Dr. Shariati Ave, Tehran, Iran

Abstract—A novel microstrip array antenna based on the meta-material zeroth-order resonator (ZOR) is presented in this paper. Considering both zeroth-order resonance and the array theory, a resonant array antenna has been designed and fabricated which has small dimensions both in length and width as well as an acceptable gain. Since the resonant frequency of the zeroth-order resonator is independent of the physical length of the resonator and determined only by LC values loaded in the resonator, therefore, antenna size can be reduced arbitrarily with no changes in the operation frequency and due to the array structure antenna gain can be enhanced. Additional benefit of the ZOR antennas is lower ohmic losses as compared to the other small antennas and hence the efficiency of the antenna is higher. The discrepancy between simulation and measurement determined by fabricating some of the simulated design and comparison between the results, has been taken into account for designing the final array. A small-sized two-elements ZOR array antenna with 50% reduction in size as compared to the conventional array with a acceptable gain and broad radiation pattern is tested at 4.25 GHz. The proposed antenna has application in radio altimeters. The commercial softwares such as CST and HFSS were utilized for design and analysis of the structure.

1. INTRODUCTION

Meta-materials or left-handed materials (LHM) are characterized by simultaneously negative permittivity (ε) and permeability (μ) in a certain frequency band. Though LHM has not been found in the nature so far, recently, researches demonstrated the practical realization of

Corresponding author: A. A. Fashi (azimi@ee.kntu.ac.ir).

LHM with left-handed transmission lines (LH TLs) [1]. The left-handed TL support backward waves in which phase velocity and group velocity have opposite signs. It can be shown that the dual of the simple transmission line shown in Fig. 1(a) supports backward waves. The phase propagation constant (for loss-less case) can be expressed as following:

$$\beta(\omega) = -1/\omega\sqrt{L_L C_L} \tag{1}$$

Therefore, the propagation phase velocity and group velocity are as follows:

$$v_p = -\omega^2\sqrt{L_L C_L}, \quad v_g = +\omega^2\sqrt{L_L C_L} \tag{2}$$

It is seen that, the phase and group velocity are anti-parallel. Since a real LH structure necessarily includes parasitic series inductances (L'_R) and shunt capacitances (C'_R) as shown in Fig. 1(b), a purely LH (PLH) structure does not exist, even in a restricted frequency range. The practical LH TL consists of the combination of a conventional right-handed (RH) TL and its dual, the LH TL, forming a "composite right/left-handed" (CRLH) TL [2]. At high frequencies, the essential characteristics of a CRLH TL is similar to a PRH TL, while at low frequencies, it is similar to a PLH. The average cell size of the CRLH TL should be at least smaller than a quarter of wavelength to ensure that TL is an effectively homogeneous structure [2–6]. Microwave applications with unusual properties have been proposed and implemented based on the CRLH TL theory [2, 7–10]. One of the applications of the CRLH structures is zeroth-order resonator (ZOR) [2] in which the CRLH TL supports an infinite wavelength at a finite microwave frequency, i.e., the voltage or currents distribution

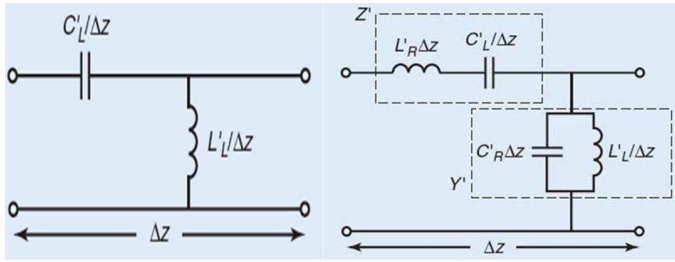

Figure 1. Equivalent circuits for meta-materials TLs. (a) Pure left-handed TL. (b) The CRLH TL with a parasitic series inductance and a shunt capacitance.

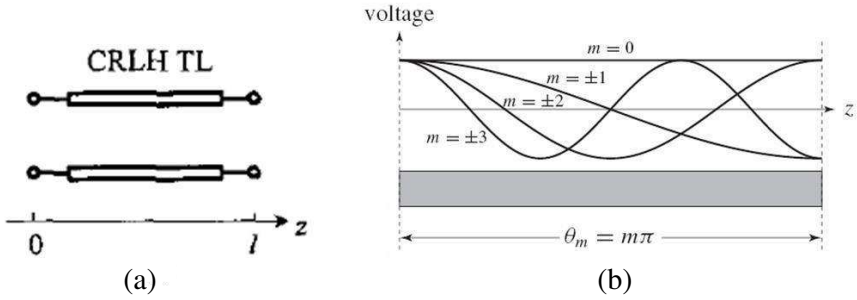

Figure 2. Resonant modes in an open-ended CRLH TL. (a) Open-ended ideal homogeneous CRLH TL. (b) Resonant modes of the open-ended CRLH TL resonator.

are uniform in the entire structure. When a CRLH TL is open-ended as shown in Fig. 2(a), standing waves and resonances are produced due to the open boundary condition where $l = m\lambda/2$ or $\theta_m = \beta_m l = m\pi$ in which l is the physical length of the resonator and m is the mode number (see Fig. 2(b)) [11]. The real CRLH TL, which consists of unit cells, can resonate at the zeroth-order mode ($m = 0$) with an infinite wavelength as well as $m = \pm 1, \pm 2, \ldots \pm (N-1)$ modes in which N is the number of unit cells. The zeroth-order resonant frequency depends only on the circuit elements of the unit cell and not on the physical length l of the resonator, thus a zeroth-order resonator could be made arbitrary small. When the zeroth-order resonator is used as a resonant antenna, since the operation frequency is independent of the physical length, there is one degree of freedom in antenna design in terms of either radiation pattern or gain, which will be an advantage of the zeroth-order resonating antenna. In this paper, a novel ZOR array antenna based on the CRLH TL is proposed and demonstrated. A small-sized array antenna with two five-unit-cell ZOR elements using microstrip structure is designed and implemented at 4.25 GHz and measured results have been compared with those obtained through the simulation. The fabricated antenna has a small size with an acceptable gain. Since the resonant frequency of the zeroth-order resonator is independent of the physical length of the resonator, antenna size can be reduced arbitrarily with no changes in the operation frequency. In addition, the ZOR fabricated antenna has lower ohmic losses as compared to the other small antennas and hence the efficiency of the antenna is higher. Moreover, the resonant frequency of the proposed antenna is within the proper frequency band of the altimeters (4.2–4.4 GHz) and can be used practically in the radio altimeters.

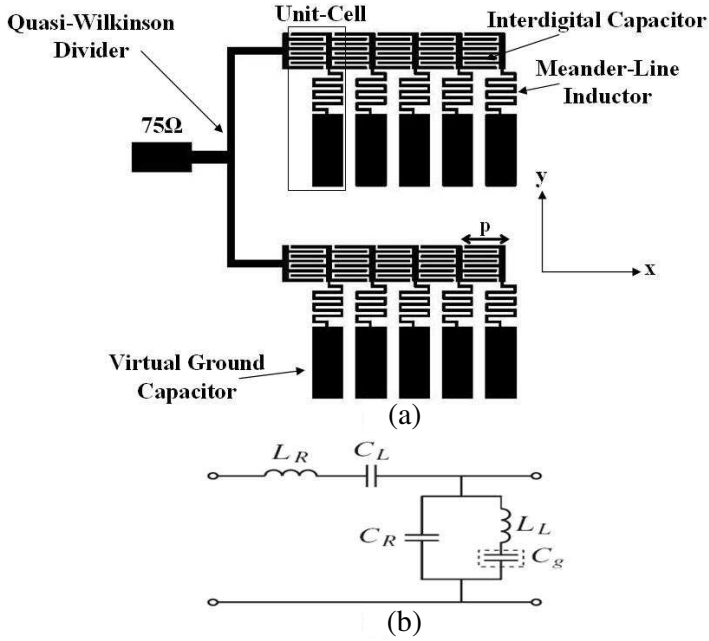

Figure 3. Microstrip ZOR array antenna implementation. (a) Circuit pattern. (b) Loss-less equivalent circuit of the unit cell.

2. ZEROTH-ORDER RESONATOR ARRAY ANTENNA

Figure 3(a) shows the proposed two-elements ZOR array antenna implemented with microstrip technology. Each of the ZOR elements consists of sequentially connected unit cells each of which has a series interdigital capacitor and a shunt meander line inductor connected to a patch. When the virtual ground patch capacitor is large, the reactance of the total shunt branch in the unit cell becomes inductive [2] and equivalent circuit of the CRLH unit cell can be shown as in Fig. 1(b). The loss-less equivalent circuit for unit cell of the proposed structure shown in Fig. 3(b). The dispersion relation of the equivalent circuit shown in Fig. 3(b) can be expressed as following [2]:

$$\beta = \frac{1}{p}\cos^{-1}\left\{1 - \frac{1}{2}\left[\frac{\omega_L^2}{\omega^2}\zeta + \frac{\omega^2}{\omega_R^2} - \left(\frac{\omega_{sh}^2}{\omega_R^2}\zeta + \frac{\omega_{se}^2}{\omega_R^2}\right)\right]\right\} \tag{3}$$

where

$$\zeta = \frac{\omega^2}{\omega^2 - \omega_g^2} \tag{4}$$

and $\omega_L = 1/\sqrt{L_L C_L}$, $\omega_R = 1/\sqrt{L_R C_R}$, $\omega_{se} = 1/\sqrt{L_R C_L}$, $\omega_{sh} = 1/\sqrt{L_L C_R}$ and $\omega_g = 1/\sqrt{L_L C_g}$. In addition, β is the phase constant and p is the period of the unit cell. $\omega - \beta$ diagram for CRLH TL based on (3) is shown in Fig. 4 [11], resonances occur when:

$$\beta_m = \frac{m\pi}{l} \quad (m = 0, \pm 1, \pm 2, \ldots, \pm(N-1)) \tag{5}$$

where N is the number of unit cells in the resonator and is obtained as:

$$N = l/p \tag{6}$$

The resonant frequencies (ω_m) are sampled at a rate of π/l along β axis on the dispersion curve as shown by the dots in Fig. 4. By choosing $\beta = 0$ in the input impedance of the open-ended CRLH TL shown in Fig. 3, one can obtained the zeroth-order resonant frequency of the structure as:

$$\omega_{res}^{open} = \sqrt{\omega_{sh}^2 + \omega_g^2} \tag{7}$$

For the short-ended CRLH resonator, the zeroth-order resonant frequency becomes:

$$\omega_{res}^{short} = \omega_{se} \tag{8}$$

In the zeroth-order resonator, for both configuration (open- and short-ended), the resonance frequency depends only on the circuit

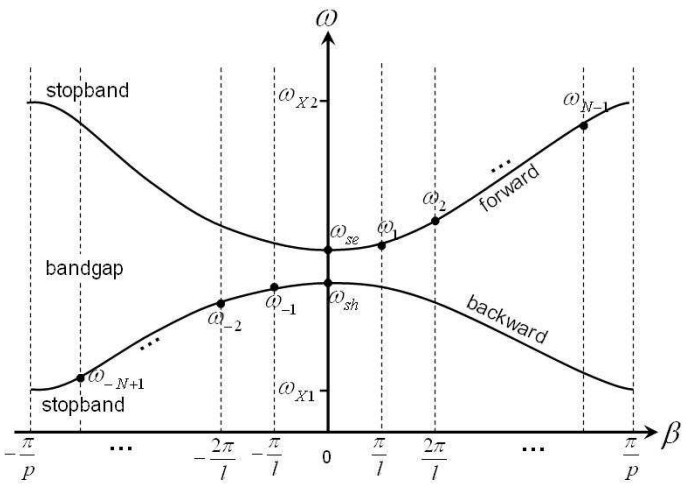

Figure 4. Typical dispersion diagram of the CRLH TL. The resonant frequencies of a open-ended or short-ended CRLH TL resonator are specified with dots on the $v_g > 0$ branch. ($\omega_{se} > \omega_{sh}$).

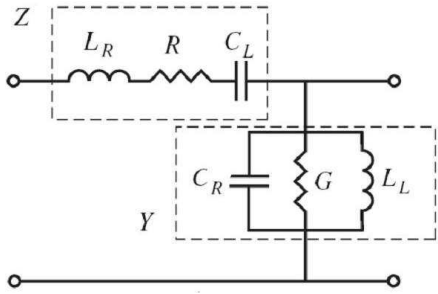

Figure 5. Equivalent circuit model for the lossy unit cell.

elements of the unit cell and the physical length of the resonator has no effect on it as in (7) and (8). In the balanced case where $\omega_o = \omega_{se} = \omega_{sh}$, the zeroth-order resonance occurs for both open-ended and short-ended resonators. In a real open-ended zeroth-order resonator with N lossy unit cell as shown in Fig. 5, the unloaded Q-factor is given by [2]:

$$Q_o^{open-ended} = \frac{1}{G}\sqrt{\frac{C_L}{L_R}} \tag{9}$$

It is noted that the unloaded Q-factor depends only on G (loss) in the shunt circuit and not on R in the series circuit of the unit cell, thus ZOR antennas have lower ohmic losses and thereby higher efficiency with respect to the other conventional small antennas.

3. IMPLEMENTATION

A ZOR array antenna with two 5-cell elements of Fig. 3(a) is fabricated on Taconic TLY-5 substrate with a thickness of 1.57 mm and relative permittivity $\varepsilon_r = 2.2$. The period of the unit cell p is 3.68 mm and a quarter of guided wavelength at operation frequency is about 11.5 mm, therefore, effective homogeneous condition is satisfied. The width of the interdigital electrodes is 0.182 mm and the space between them is 0.218 mm. The number of electrodes is 8 and the width of meander lines is 0.182 mm. The virtual ground plane size is $6 \times 2.54\,\text{mm}^2$. The ZOR elements are fed uniformly by a quasi-wilkinson power divider in which the input line size is $3 \times 1\,\text{mm}^2$ connected to the 75 Ω line with length of 4 mm and size of the output lines is about $12.5 \times 0.6\,\text{mm}^2$. Since the width of the 50 Ω line is large (about 4.8 mm) which can cause undesired radiation, 75 Ω line is used. The length of the output lines is about one quarter of guided wavelength and the characteristics

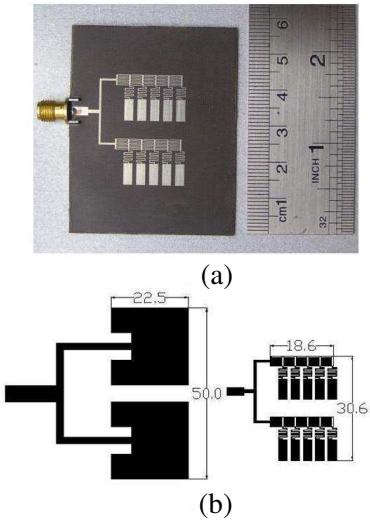

Figure 6. (a) Fabricated two-elements ZOR array antenna (f = 4.25 GHz). (b) Footprint area of the ZOR array compared with a conventional two-elements array at the same frequency.

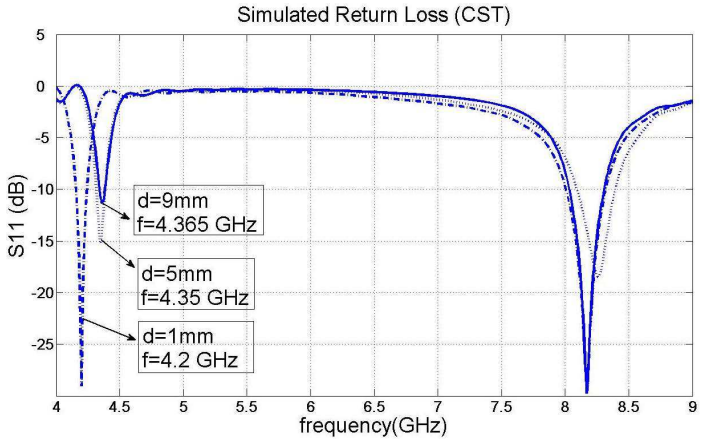

Figure 7. Simulated $|S_{11}|$ of the proposed ZOR array antenna for the different spaces between elements.

impedance of the each output lines is almost 1.2 times that of the input line. Fig. 6(a) shows the fabricated ZOR array antenna. The foot-print area reduced about 50% compared with a $\lambda/2$ conventional array antenna on the same substrate as shown in Fig. 6(b).

3.1. The Space between Array Elements

The mutual coupling between array elements is an important factor and should be controlled by the space between two elements. As shown in Fig. 7, mutual coupling is increased with the space reduction and therefore operation frequency is changed greatly. By increasing separation although mutual coupling and frequency shift decrease but the array size increases. In our design, an optimum spacing of 5 mm is considered because for the spaces more than 5 mm, variation of the resonant frequency and thereby mutual coupling is negligible (Fig. 7).

3.2. Increasing Number of the Unit Cells

By increasing the number of cells in a ZOR antenna physical length and gain of the antenna increases with no changes (in theory) in operation frequency, but in this method for gain enhancement the antenna size increases asymmetrically and it is not desired. Fig. 8(a)

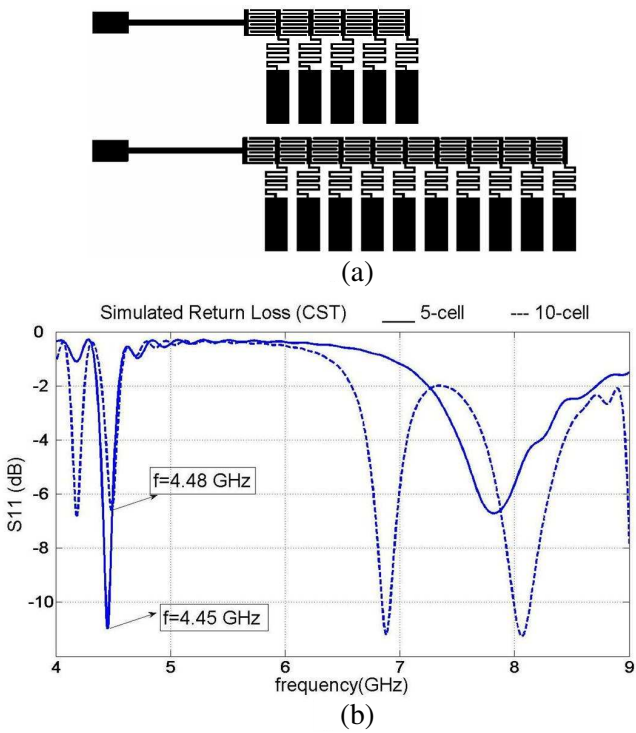

Figure 8. Simulated $|S_{11}|$ of the single 5-cell ZOR antenna compared with the single 10-cell ZOR antenna.

shows a single 5-cell and a single 10-cell ZOR antenna with the same unit cells proposed in previous sections. Simulated input return loss for these antennas is shown in Fig. 8(b). As shown in Fig. 9(b), discrepancy between the operation frequency of 5-cell and 10-cell antenna is negligible. The simulated gain is about 6 dB for 10-cell antenna and 4.3 dB for 5-cell antenna. The dispersion diagram of the 5-cell element of the fabricated array has been simulated with CST software and shown in Fig. 9. It is important to note that dispersion diagram of the 5-cell element is equal to the dispersion diagram of the array.

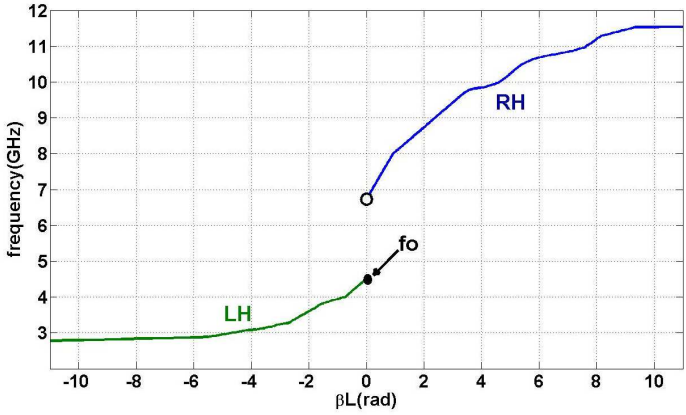

Figure 9. Simulated dispersion diagram of the 5-cell element using CST software ($L = 5p$).

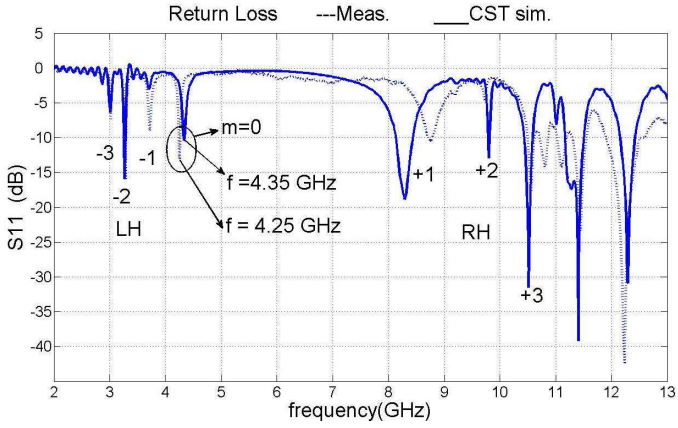

Figure 10. Measured and simulated $|S_{11}|$ of the prototype ZOR array antenna.

4. SIMULATION AND MEASUREMENT RESULTS

Figure 10 shows the simulation and experiment results for $|S_{11}|$ at the input port of the array. The measured zeroth-order resonant frequency is at 4.25 GHz and the simulated zeroth-order resonant frequency is at 4.35 GHz, therefore, the discrepancy between the simulation and fabrication for the resonant frequency is about 100 MHz. The 4.2–4.4 GHz frequency band is allocated to aeronautical radio navigation services and fabricated antenna can be used in radio altimeters. Negative mode resonant frequencies are below the zeroth-order resonant frequency in the left-handed frequency band. In this

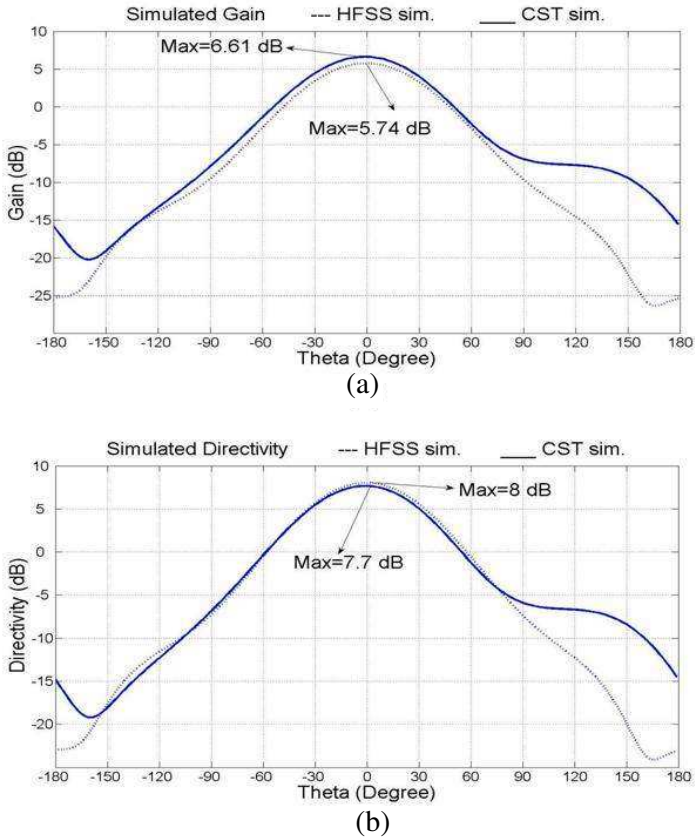

Figure 11. The variation of the simulated (CST, HFSS) gain and directivity of the array antenna with θ in the plane $\varphi = 90$ at simulated resonant frequency (4.35 GHz).

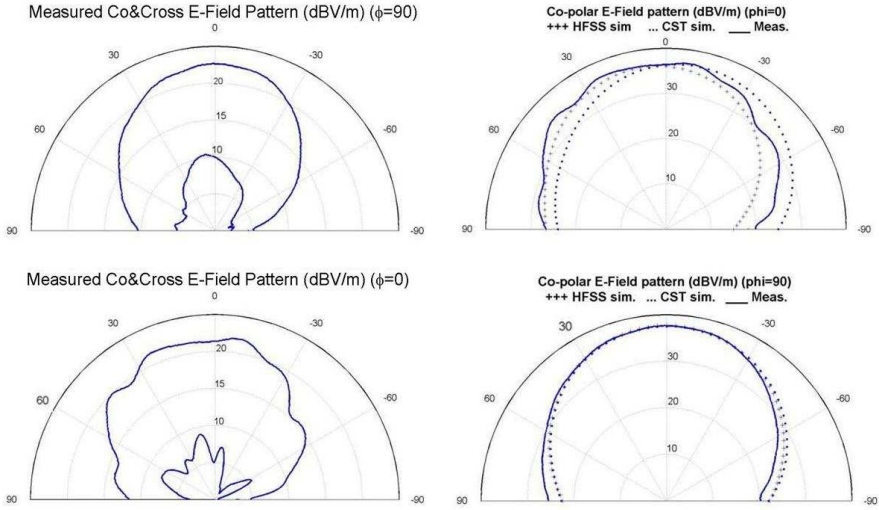

Figure 12. Measured and simulated 2D radiation patterns of the the prototype ZOR array antenna.

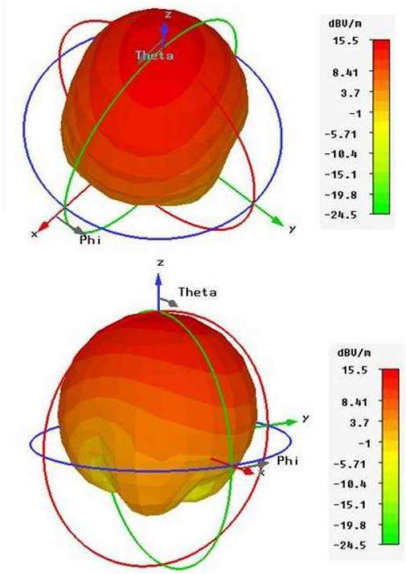

Figure 13. Simulated 3D radiation patterns of the the prototype ZOR array antenna.

structure $\omega_{sh} < \omega_{se}$, therefore, in the $|S_{11}|$ diagram, the first resonant frequency in the left of the bandgap is the ZOR frequency. The positive mode resonant frequencies are above the bandgap in the right-handed region. The simulated antenna gain and directivity in terms of the angle θ is shown in Fig. 11. Using the CST results, gain of the array is about 6.6 dB at resonant frequency. Antenna efficiency is almost 80% which is higher than the other small conventional antennas.

Figure 12 showes measured and simulated 2D radiation patterns of the ZOR array antenna at its operation frequency of 4.25 GHz. As shown in Figs. 10 and 12, the measured results agree well with simulated results and broad directivity with no undesired side lobes is obtained. Measured return loss at resonant frequency is about -13 dB and cross-polar level is within the acceptable range. The simulated 3D radiation patterns are shown in Fig. 13.

5. CONCLUSION

A novel microstrip small-sized ZOR array antenna has been presented. The operation frequency is determined only by reactances loaded in the unit cell and not by the physical length of the resonators. A small-sized and enhanced gain ZOR antenna with 50% reduction in effective size as compared to a conventional array with a broad directivity is demonstrated at 4.25 GHz. The proposed antenna can be used in the radio altimeters and has a higher efficiency with respect to the other small conventional antennas.

ACKNOWLEDGMENT

This work is supported by Iran Telecommunication Research Center.

REFERENCES

1. Li, Y. and S. Xu, "A novel microstrip antenna array fed with CRLH-TL structure," *IEEE Antenna and Propagation Society International Symposium*, 4153–4156, Jul. 2006.
2. Caloz, C. and T. Itoh, *Electromagnetic Metamaterials: Transmission Line Theory and Microwave Applications*, John Wiley & Sons, Inc., 2006.
3. Qi, Z. and L. Huan, "Design of printed antenna with left-handed array," *2005 Asia-Pacific Microwave Conference (APMC) Proceedings*, Vol. 4, 3, Dec. 2005.

4. Caloz, C. and T. Itoh, "Application of the transmission line theory of the left-handed (LH) materials to the realization of a microstrip LH transmission line," *IEEE-APS Int'l Symp. Digest*, Vol. 2, 412–415, Jun. 2002.
5. Oliner, A. A., "A periodic-structure negative-refractive-index medium without resonant elements," *IEEE-APS/URSI Int'l Symp. Digest*, 41, Jun. 2002.
6. Eleftheriades, G. V., A. K. Lyer, and P. C. Kremer, "Planar negative refractive index media using periodically L-C loaded transmission lines," *IEEE Trans. on Microwave Theory Tech.*, Vol. 50, No. 12, 2702–2712, Dec. 2002.
7. Sanada, A., C. Caloz, and T. Itoh, "Characteristics of the composite right/left-handed transmission lines," *IEEE Microwave and Wireless Component Letters*, Vol. 14, No. 2, 68–70, Feb. 2004.
8. Caloz, C., A. Sanada, and T. Itoh, "A novel composite right/left-handed coupled-line directional coupler with arbitrary coupling level and broad bandwidth," *IEEE Microwave Theory and Thechniques*, Vol. 52, No. 3, 980–992, Mar. 2004.
9. Sanada, A., C. Caloz, and T. Itoh, "Planar distributed structures with negative refractive index," *IEEE Microwave Theory and Techniques*, Vol. 52, No. 4, 1252–1263, Apr. 2004.
10. Sanada, A., C. Caloz, and T. Itoh, "Novel zeroth-order resonance in composite right/left-handed transmission line resonator," *2003 Asia-Pacific Microwave Conference Proceedings*, 1588–1591, Nov. 2003.
11. Sanada, A., M. Kimura, I. Awai, C. Caloz, and T. Itoh, "A planar zeroth-order resonator antenna using a left-handed transmission line," *2004 European Microwave Conference*, Vol. 3, 1341–1344, Oct. 2004.
12. Fashi, A. A., M. Kamyab, and M. Barati, "A novel small resonant antenna using the meta-materials array," *PIERS Proceedings*, 670–674, Moscow, Russia, Aug. 2009.
13. Barati, M., M. Kamyab, and A. A. Fashi, "Beam steering capability based on microstrip CRLH transmission line," *PIERS Proceedings*, 657–661, Moscow, Russia, Aug. 2009.